The HKU Scholars Hub   The University of Hong Kong   香港大學學術庫

Title	**Hunting for Orphaned Central Compact Objects Among Radio Pulsars**
Author(s)	**Luo, J; Ng, SCY; Ho, WCG; Bogdanov, S; Kaspi, VM; He, C**
Citation	**The Astrophysical Journal, 2015, v. 808 n. 2, article no. 130**
Issued Date	**2015**
URL	**http://hdl.handle.net/10722/214491**
Rights	

HUNTING FOR ORPHANED CENTRAL COMPACT OBJECTS AMONG RADIO PULSARS

J. Luo[1], C.-Y. Ng[1], W. C. G. Ho[2], S. Bogdanov[3], V. M. Kaspi[4], and C. He[5]

ApJ, in press

ABSTRACT

Central compact objects (CCOs) are a handful of young neutron stars found at the center of supernova remnants (SNRs). They show high thermal X-ray luminosities but no radio emission. Spin-down rate measurements of the three CCOs with X-ray pulsations indicate surface dipole fields much weaker than those of typical young pulsars. To investigate if CCOs and known radio pulsars are objects at different evolutionary stages, we carried out a census of all weak-field ($< 10^{11}$ G) isolated radio pulsars in the Galactic plane to search for CCO-like X-ray emission. None of the 12 candidates are detected at X-ray energies, with luminosity limits of $10^{32} - 10^{34}$ erg s^{-1}. We consider a scenario in which the weak surface fields of CCOs are due to a rapid accretion of supernova materials and show that as the buried field diffuses back to the surface, a CCO descendant is expected to leave the P-$\dot{P}$ parameter space of our candidates at a young age of a few $\times 10$ kyr. Hence, the candidates are likely to just be old ordinary pulsars in this case. We suggest that further searches for orphaned CCOs, which are aged CCOs with parent SNRs that have dissipated, should include pulsars with stronger magnetic fields.

Subject headings: pulsars: general — stars: evolution — stars: neutron — X-rays: stars

1. INTRODUCTION

Before the mid-1990s it was believed that young neutron stars are all fast-spinning objects with high surface magnetic field strengths of $\sim 10^{12}$ G, emitting radio pulses. However, recent discoveries of new populations of neutron stars, including central compact objects (CCOs), magnetars, and X-ray dim isolated neutron stars, have challenged this simple picture (see reviews by Kaspi 2010; Harding 2013). CCOs are the most enigmatic class. They are found at the center of supernova remnants (SNRs) and cannot be as easily classified as other types of objects. There are nine confirmed CCOs sharing the following properties: (1) they are located near the centers of young SNRs; (2) they show no radio or optical counterparts; (3) they have no detectable pulsar wind nebulae; and (4) they exhibit a thermal spectrum in the soft X-ray band with high luminosity $\gtrsim 10^{33}$ erg s^{-1} (see de Luca 2008; Gotthelf & Halpern 2008; Gotthelf et al. 2013a, for reviews). Since CCOs are generally associated with very young SNRs, their nature and evolution are highly relevant to the neutron star production rate and the physics underlying the branching ratios of core collapse (Keane & Kramer 2008). However, the active lifetime and evolution of CCOs are poorly understood due to the small sample. It is also unclear if these neutron stars are intrinsically radio-quiet, or if they are radio pulsars beamed away from us (see e.g., Ho 2013b).

Only three CCOs have X-ray pulsations firmly detected. They show periods of $P = 0.1$–0.4 s and long-term timing revealed small period derivatives of $\dot{P} \approx 10^{-17}$ (Halpern & Gotthelf 2010; Gotthelf et al. 2013a). Their spin parameters are plotted in the P-$\dot{P}$ diagram in Figure 1. These suggest spin-down luminosities of $\dot{E} \equiv 4\pi^2 I \dot{P}/P^3 = 10^{31}$–$10^{32}$ erg s^{-1}, where I is the neutron star moment of inertia. These values are nearly two orders of magnitude smaller than the CCO's X-ray luminosities, implying that the sources cannot be entirely powered by rotation. The characteristic age $\tau_c = P/2\dot{P}$ of the three CCOs is over 10^8 years, much older than their true ages of a few thousand years, estimated from their associated SNRs. The inferred surface dipole field strengths $B \equiv 3.2 \times 10^{19}(P\dot{P})^{1/2}$ G are of the order of 10^{10} G. These are much lower than those of young pulsars but still lie well above the radio pulsar "death line" (e.g., $B/P^2 \simeq 1.7 \times 10^{11}$ G s^{-2}; Bhattacharya et al. 1992), which is the (uncertain) theoretical limit for producing radio emission. Indeed, radio pulsars have been detected in the CCO range of P and $\dot{P}$ (see Figure 1), hence with comparable dipole field strengths. This raises a fundamental question: are CCOs and radio pulsars the same class of objects or do they belong to disjointed sets of neutron stars?

If CCOs are ordinary radio pulsars born with weak magnetic fields (see, e.g., Bonanno et al. 2006; Spruit 2008), their small $\dot{P}$ values imply very slow spin evolution, such that they take a long time to reach the death line. The detection of nine young CCOs implies that there should be over 10^6 older ones in the Galaxy (Kaspi 2010). This is in contrast to the small number of known radio pulsars with low $B \sim 10^{10}$ G as shown in the P-$\dot{P}$ diagram in Figure 1, given that there is no observational bias against these pulsars in radio surveys (see Kramer et al. 2003; Faucher-Giguère & Kaspi 2006). The discrepancy could be reconciled if CCOs are strong-field objects but appear to have weak surface fields at a young age. This is supported by modeling of CCOs'

[1] Department of Physics, the University of Hong Kong, Hong Kong; ncy@bohr.physics.hku.hk
[2] Mathematical Sciences and STAG Research Centre, University of Southampton, Southampton SO17 1BJ, UK
[3] Columbia Astrophysics Laboratory, Columbia University, New York, NY 10027, USA
[4] Department of Physics and McGill Space Institute, McGill University, Montreal, QC H3A 2T8, Canada
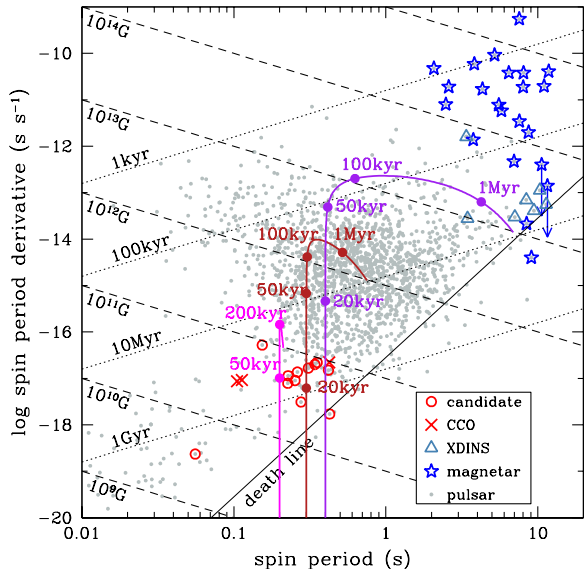[5] Department of Physics, the University of Chicago, Chicago, IL 60637, USA

FIG. 1.— Pulsar P-$\dot{P}$ diagram showing our orphaned CCO candidates and other types of neutron stars. The solid curves show the theoretical evolution of stars with buried magnetic fields at birth (see Section 3 for details). From left to right, the initial surface B-field strengths are 10^{12} G (pink), 10^{13} G (brown), and 10^{14} G (purple), and the initial spin periods are set to 0.2, 0.3, and 0.4 s, respectively, for clarity. Selected time points are marked.

X-ray light curves, which suggest a strong crustal field (Gotthelf et al. 2010; Shabaltas & Lai 2012; Bogdanov 2014). It was proposed that the B-fields of CCOs could be buried by supernova fallback (Halpern & Gotthelf 2010; Ho 2011, 2013a), and hence the radio emission is suppressed (as in the case of accreting millisecond pulsars in quiescence; see e.g., Stappers et al. 2014; Archibald et al. 2015). After accretion stops, the B-field is expected to diffuse back to the surface with a timescale depending sensitively on the amount of accreted mass and ranging from 10^3 years to over 10^6 years (see Chevalier 1989; Geppert et al. 1999; Ho 2011; Viganò & Pons 2012). The radio emission would then presumably switch on (Muslimov & Page 1996). This picture predicts that young CCOs should be radio-quiet and aged ones could become ordinary radio pulsars (see Gotthelf et al. 2013b; Bogdanov et al. 2014).

No radio emission has yet been observed from any CCO (see Pavlov et al. 2004, and references therein), but given the small number of known pulsating CCOs and the possibility of small beaming fractions, the result is inconclusive and a more systematic study is needed. In addition to deeper radio observations, we can turn the search around to look for CCO-like X-ray emission from selected weak-field radio pulsars. Indeed, if CCOs manifest as radio pulsars, this could be a more efficient way to detect them, especially after their natal SNRs fade away in $\sim 10^5$ years. Any detection of X-ray emission from the radio-selected sample will confirm CCOs as a subset of radio pulsars, providing direct evidence to rule out the scenario of ongoing accretion. There were previous attempts to identify CCOs from radio pulsars positionally coincident with SNRs (Bogdanov et al. 2014) and aged CCOs with parent SNRs that have dissipated (so-called orphaned CCOs) from disrupted recycled pulsars

(Gotthelf et al. 2013b). However, no new CCOs have been found. To complete the study, here we present an X-ray census of all isolated weak-field radio pulsars near the Galactic plane to search for CCO-like emission. The sample selection and data analysis are described in Section 2 and we report the detection limits and discuss the implications in Section 3.

2. OBSERVATIONS AND DATA REDUCTION

We select weak-field radio pulsars from the ATNF catalog (Manchester et al. 2005) with similar spin parameters as those of the known CCOs, according to the following criteria:

1. weak surface dipole B-fields of $B \leq 10^{11}$ G inferred from spin-down;

2. isolated and having periods $P \geq 0.05$ s to avoid recycled pulsars; and

3. located < 100 pc from the Galactic plane to exclude old objects.

The pulsar height from the plane is calculated from the source's Galactic latitude and estimated distance. Neutron stars are born at an average distance of 50 pc from the plane with a mean space velocity of ~ 350 km s^{-1} (Faucher-Giguère & Kaspi 2006). At this velocity, a pulsar travels only 36 pc in 10^5 years, which is well below the cut even in the rare case that a pulsar moves exactly perpendicular to the plane.

Our sample consists of 12 candidates. They are plotted in the P-$\dot{P}$ diagram in Figure 1 and their properties are listed in Table 1. While the pulsars have large characteristic ages of $\sim 10^8$ years, we note that their true age could be much younger, particularly if they were born spinning slowly (see Ng et al. 2007; Bogdanov et al. 2014). There is an archival *Chandra* on-axis ACIS-S observation of PSR J1355−6206 with 3 ks exposure, and PSR J1755−2725 was located far off-axis in two *Chandra* ACIS-I exposures with a total of 4 ks. PSR J1819−1510 falls onto the edge of the field of view in two *XMM-Newton* MOS exposures. After filtering the background flaring periods and correcting for vignetting, we obtained an effective total exposure of 72 ks for this source. The *XMM-Newton* PN data were not used in this study, as the total exposure is only 21 ks. For the remaining nine candidates, we obtained *Chandra* ACIS-S observations with 5 ks exposure each, except for PSRs J1702−4217 and J1650−4341, which have roughly 8 ks each. The observation IDs (ObsIDs) and effective exposures are listed in Table 2. Note that observations of three sources: PSRs J0609+2130, J1355−6206, and B1952+29 were recently reported in an independent study (Gotthelf et al. 2013b).

We carried out standard *Chandra* data reduction with CIAO v4.5 and CALDB v4.5.8. We reprocessed the data using the task `chandra_repro` and checked that there was no background flaring occuring during the *Chandra* observations; all data are therefore used in the analysis. The *XMM-Newton* data reduction was performed with SAS v13.5[6]. We used the task `emchain` to reprocess the

---

[6] *XMM-Newton* SAS is developed and maintained by the Science Operations Centre at the European Space Astronomy Centre and the Survey Science Centre at the University of Leicester.

TABLE 1
Properties of Orphaned CCO Candidates

Pulsar	Dist.[a] (kpc)	l (°)	b (°)	DM ($10\,\mathrm{pc\,cm^{-3}}$)	N_{H}[b] ($10^{22}\,\mathrm{cm^{-2}}$)	P (s)	$\dot{P}$ (10^{-18})	τ_c[c] (10^8 years)	B[d] (10^{10} G)
J0609+2130	1.2	189.2	1.0	3.9	$0.12^{+0.09}_{-0.04}$	0.06	0.24	38	0.37
J1107−5907	1.3	289.9	1.1	4.0	$0.12^{+0.09}_{-0.04}$	0.25	9.0	4.5	4.8
J1355−6206	8.3	310.3	−0.2	55	$1.7^{+1.2}_{-0.5}$	0.28	3.1	14	3.0
J1425−5723	1.2	315.4	3.2	4.3	$0.13^{+0.1}_{-0.04}$	0.35	22	2.5	8.9
J1650−4341	7.5	341.6	0.5	67	$2.1^{+1.5}_{-0.7}$	0.31	17	2.9	7.3
J1653−4315	4.6	342.3	0.4	34	$1.0^{+0.7}_{-0.3}$	0.42	15	4.4	8.0
J1702−4217	7.1	344.1	−0.3	63	$1.9^{+1.4}_{-0.6}$	0.23	11	3.2	5.2
J1739−3951	0.8	4.0	−4.7	2.5	$0.076^{+0.05}_{-0.02}$	0.34	20	2.7	8.3
J1755−2725	2.4	2.4	−1.1	12	$0.35^{+0.25}_{-0.10}$	0.26	14	3.0	6.1
J1810−1820	5.6	12.1	0.3	45	$1.4^{+1.0}_{-0.5}$	0.15	52	0.47	9.1
J1819−1510	5.3	15.9	−0.1	42	$1.3^{+0.9}_{-0.4}$	0.23	7.9	4.6	4.3
B1952+29	0.7	65.3	0.8	0.79	$0.024^{+0.017}_{-0.008}$	0.43	1.7	40	2.7

[a] All distance are estimated from the DM, since no parallax measurements are available.
[b] N_{H} values are estimated by $N_{\mathrm{H}}\,(10^{20}\,\mathrm{cm^{-2}}) = 0.30^{+0.13}_{-0.09}\,\mathrm{DM}\,(\mathrm{pc\,cm^{-3}})$ (He et al. 2013).
[c] The characteristic age is given by $\tau_c \equiv P/2\dot{P}$.
[d] The surface magnetic field strength, B, is inferred from the spin parameters with $B \equiv 3.2 \times 10^{19}(P\dot{P})^{1/2}\,\mathrm{G}$, where P is in seconds.

TABLE 2
Flux and Age Limits of the Orphaned CCO Candidates

Pulsar	ObsID[a]	Effective Exposure (ks)	Count Rate Upper Limit[b] ($10^{-4}\,\mathrm{cnt\,s^{-1}}$)	kT_{max}[c] (eV)	$L_{\mathrm{max}}^{\mathrm{bol}}$[c] ($10^{33}\,\mathrm{erg\,s^{-1}}$)	Age Lower Limit[d] (kyr)
J0609+2130	12687	5	6.3	51	$0.18^{+0.04}_{-0.02}$	20
J1107−5907	12688	5	14	55	$0.25^{+0.06}_{-0.02}$	20
J1355−6206	13806	3.4	9.1	134	$8.7^{+8.4}_{-0.9}$	⋯
J1425−5723	12686	5	8.9	53	$0.21^{+0.05}_{-0.02}$	20
J1650−4341	13777	8	3.9	124	$6.4^{+5.0}_{-2.1}$	⋯
J1653−4315	13774	5	6.3	98	$2.5^{+1.9}_{-0.8}$	0.4
J1702−4217	13776	8.6	6.4	126	$6.8^{+6.3}_{-1.2}$	⋯
J1739−3951	12685	5	6.3	46	$0.12^{+0.02}_{-0.01}$	30
J1755−2725	8717, 8718	4	12	79	$1.1^{+0.5}_{-0.2}$	1
J1810−1820	13775	5	14	119	$5.5^{+4.0}_{-1.8}$	⋯
J1819−1510	0406450201, 0505240101	71.5	1.4	117	$5.1^{+3.7}_{-1.6}$	0.2
B1952+29	12684	5	6.3	45	$0.107^{+0.005}_{-0.002}$	30

[a] All are *Chandra* observations except for PSR J1819−1510, which was observed with *XMM-Newton* MOS.
[b] The count rate limits are at a 2σ (i.e., 95%) confidence level in the 0.5–7 keV energy range.
[c] The surface temperature (kT_{max}) and bolometric luminosity ($L_{\mathrm{max}}^{\mathrm{bol}}$) upper limits are inferred from the count rate limits, assuming uniform blackbody emission with an observed radius of $R_{\infty}=14.5$ km and the DM distance in Table 1. See the text for the details.
[d] The age lower limits are inferred from the bolometric luminosity using the minimal neutron star cooling scenario (see Figure 2).

MOS data, then applied filtering using standard flags and rejected periods with high background. The analysis is restricted to events with PATTERN ≤ 12. Finally, we generated X-ray images in the 0.5–7 keV energy range for source detection.

3. RESULTS AND DISCUSSION

The X-ray images show no obvious X-ray sources at the radio pulsar positions. To establish the pulsar flux limits, we extracted events from 5″ and 70″ radius source and background regions, respectively, for the 10 on-axis *Chandra* observations. The 5″ radius was chosen to ensure that the region encircles over 95% of the flux. A larger source region of 10″ radius was used for PSR J1755−2725, due to the large off-axis angle. For the *XMM-Newton* observations of PSR J1819−1510, we used a 60″ radius source region and excluded a background source inside. We follow Bogdanov et al. (2014) to compute the detection limits at a 2σ confidence level, using the task `aprates` in CIAO, which is based on Bayesian statistics. The results are reported in Table 2.

The count rate limits above can be converted to luminosity limits using a spectral model. Following Gotthelf et al. (2013b), we assume uniform blackbody emission from the entire star with an observed radius of $R_{\infty} = 14.5$ km (which corresponds to a neutron star
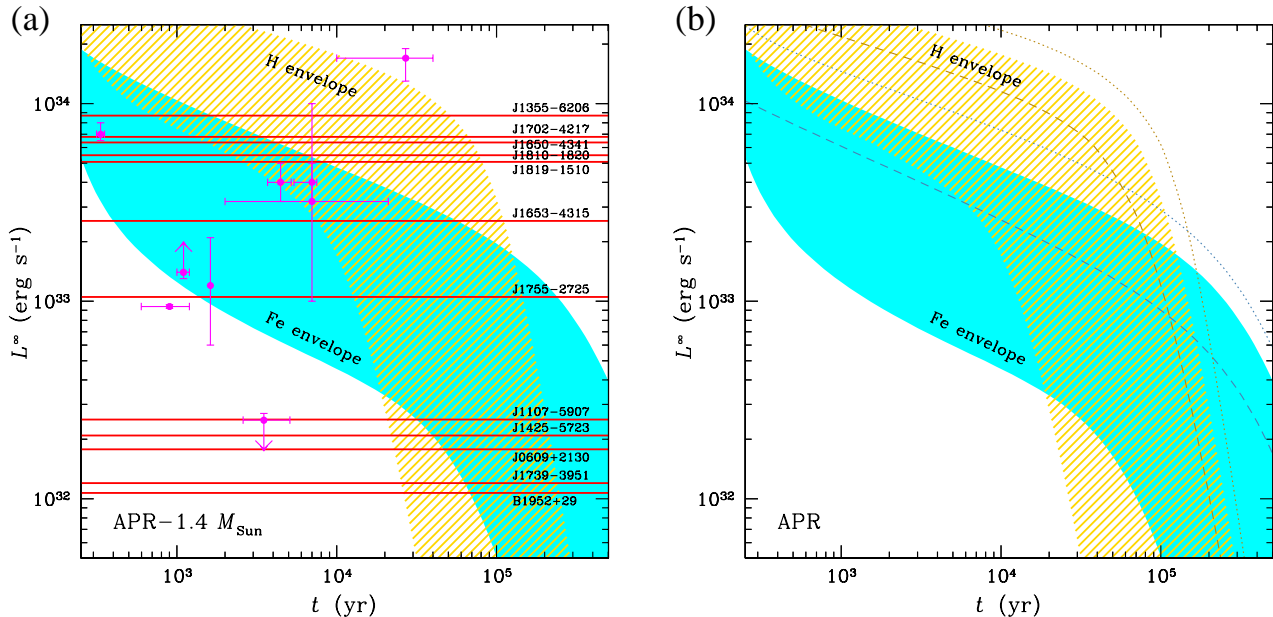
FIG. 2.— (a): Evolution of neutron star bolometric luminosity in the standard cooling scenario with $1.4\,M_\odot$, $R = 11.6\,$km (i.e., $R_\infty = 14.5\,$km for a redshift of 1.25), and hydrogen and iron envelopes (see the text for the details). For each region, the upper bound is obtained by only considering superconducting protons and the lower bound by considering superfluid neutrons as well. The red lines indicate the luminosity limits of the orphaned CCO candidates listed in Table 2. The magenta points show the age and luminosity values of confirmed CCOs, from high to low luminosity: XMMU J173203.3−344518 in HESS J1731−347 (Klochkov et al. 2015); CXOU J232327.9+584842 in Cas A (Fesen et al. 2006; Heinke & Ho 2010); CXOU J185238.6+004020 in Kes 79 (Sun et al. 2004; Viganò et al. 2013); RX J0822.0−4300 in Puppis A (Becker et al. 2012; Viganò et al. 2013); 1E 1207.4−5209 in PKS 1209−51/52 (Roger et al. 1988; Viganò et al. 2013); CXOU J160103.1−513353 in G330.2+1.0 (McClure-Griffiths et al. 2001; Park et al. 2009); 1WGA J1713.4−3949 in G347.3−0.5 (Lazendic et al. 2003; Cassam-Chenaï et al. 2004; Fesen et al. 2012); XMMU J172054.5−372652 in G350.1−0.3 (Gaensler et al. 2008; Lovchinsky et al. 2011); and CXOU J085201.4−461753 in G266.1−1.2 (Kargaltsev et al. 2002; Allen et al. 2015). (b): Cooling curves of $1.2\,M_\odot$ (dotted lines) and $1.9\,M_\odot$ (dashed lines) neutron stars calculated assuming superconducting protons only.

radius of 11.6 km for a gravitational redshift of 1.25). The pulsar dispersion measure (DM) distance is adopted and the X-ray absorption column density (N_H) is inferred from DM using the empirical relation $N_H\,(10^{20}\,cm^{-2}) = 0.30^{+0.13}_{-0.09}\,$DM $(pc\,cm^{-3})$ (He et al. 2013). We generated spectral response files for individual observations and determined the flux limits in the Sherpa environment (Freeman et al. 2001) by comparing the expected count rates with the observed limits. The surface temperature and bolometric luminosity limits are listed in Table 2. The detection limits of PSRs J0609+2130, J1355−6206, and B1952+29 are compatible with those reported in the previous study (Gotthelf et al. 2013b). As shown in the table, the luminosity limits are $\sim 10^{32}\,erg\,s^{-1}$ for nearby ($< 2\,$kpc) sources and a few times $10^{33}\,erg\,s^{-1}$ for the rest. In Figure 2, these results are compared with the observed bolometric luminosities of known CCOs. The latter are generally above $10^{33}\,erg\,s^{-1}$, suggesting that our candidates are unlikely to be young CCOs.

As mentioned, the characteristic age is not a good indicator of the true age of a pulsar. We therefore attempt to constrain the age by comparing the luminosity limits above with standard neutron star cooling curves. We employed a cooling code based on Gnedin et al. (2001) with some modifications as described in Ho et al. (2015). The temperature evolution of an isolated neutron star is determined by the relativistic equations of energy balance and heat flux (see, e.g., Yakovlev & Pethick 2004). Two important factors affecting the evolution are the composition of the outer layer (i.e., the envelope) and whether

the stellar interior is superfluid and/or superconducting. For the former, the envelope serves as a heat blanket (Gudmundsson et al. 1982). If it is composed of light elements, which have higher thermal conductivity, it would be more heat transparent (Potekhin et al. 2003). However, the exact composition of the envelope is uncertain. For the second factor, superfluidity and superconductivity suppress heat capacities and some emission mechanisms, such as modified Urca processes. On the other hand, emission due to the Cooper pairing of nucleons would be enhanced when the temperature decreases just below the critical value (see Yakovlev & Pethick 2004; Page et al. 2006, for reviews).

Here we consider a $1.4\,M_\odot$ and 11.6 km radius (corresponding to an observed radius $R_\infty = 14.5\,$km) star built with the Akmal-Pandharipande-Ravenhall (APR) equation of state (EOS) (Akmal et al. 1998) and the standard (also known as minimal) cooling scenario, in which neutrino emission by fast direct Urca processes does not take place (see, e.g., Yakovlev & Pethick 2004; Page et al. 2006). We show in Figure 2 two shaded regions, one for a maximally thick $10^{-7}\,M_\odot$ hydrogen envelope and one for an iron envelope. The upper boundary of each region is determined by a cooling model with only superconducting protons (gap model CCDK) and the lower boundary accounts for superfluid neutrons as well (singlet gap model SFB and triplet gap model TToa), which induce more rapid cooling (see Ho et al. 2015, for details). To illustrate the effect of different masses, we plot in the figure inset cooling curves of $1.2\,M_\odot$ and $1.4\,M_\odot$

stars for models with only superconducting protons.

The model cooling curves are compared with the candidates' luminosity limits in Figure 2 to constrain the source age. The result slightly depends on the neutron star mass in the model, but the main uncertainty comes from the whether or not neutrons in the core become superfluid. The inferred age lower limits are listed in Table 2. The results are not very constraining. For nearby objects that have good luminosity limits, we deduce age limits of $\sim 2 \times 10^4$ years, but no useful limits are obtained for the rest, and deeper X-ray observations are needed for further investigation. Unlike the CCO candidates in our previous study (Bogdanov et al. 2014), none of the sources here coincide with known SNRs, and we do not find evidence of remnant emission from the X-ray data. This indeed gives a hint that the sources are likely older than $\sim 10^5$ years, such that the SNRs have already dissipated in the interstellar environment.

The non-detection of X-ray emission from our sample of weak-field radio pulsars seems to support the idea that the two are not evolutionary connected classes of neutron stars, similar to what previous studies have suggested (e.g., Gotthelf et al. 2013b, Bogdanov et al. 2014). It was proposed that the magnetic fields of CCOs could be buried by accretion from supernova materials at birth (Halpern & Gotthelf 2010; Ho 2011, 2013a), resulting in the suppression of radio emission. As the field diffuses back to the surface, the radio emission would subsequently turn on so that a CCO becomes a radio pulsar. To investigate the effect of magnetic field diffusion on the neutron star spin evolution, we applied a model described in Ho (2011) to solve the induction equation. We assumed that the B-field is confined in the crust and is initially buried at a high density of $10^{13}\,\mathrm{g\,cm^{-3}}$, which corresponds to a depth of $\sim 400\,\mathrm{m}$ or an accreted mass of $\sim 5 \times 10^{-4}\,M_\odot$ (see Ho 2011). We consider different initial surface B-field strengths from $10^{12}\,\mathrm{G}$ to $10^{14}\,\mathrm{G}$ and the resulting spin evolution is overplotted in the P-$\dot{P}$ diagram in Figure 1. We found that even at this large burial depth, the field emerges with a relatively short timescale of a few $\times 10^4$ years, resulting in a vertically upward track in the diagram. More importantly, a CCO with an emerging surface field is expected to pass through the P-$\dot{P}$ parameter space of our candidates (i.e., $B \approx 10^{10}$–$10^{11}\,\mathrm{G}$) at a young age of the order of $10^4\,\mathrm{yr}$, such that it should remain hot and luminous, with the parent SNR probably still visible. If this model is true, our candidates are likely to just be old ordinary pulsars rather than orphaned CCOs. Moreover, we expect that when an aged CCO turns on as a radio pulsar, it will have a stronger B-field than those of our candidates.

For further study, identifying CCO descendants would require X-ray observations of more radio pulsars to search for thermal emission (see also Gotthelf et al. 2013b). In particular, it would be useful to extend the survey to include sources with $B \gtrsim 10^{11}\,\mathrm{G}$. On the other hand, it is

more difficult to detect an orphan CCO if the radio emission never turns on (see Halpern et al. 2013). This is best done with all-sky surveys in X-rays, such as the upcoming *eROSITA* mission (Merloni et al. 2012). Finally, pulsar braking index measurements from long-term timing could reveal a growing dipole field (e.g., Espinoza et al. 2011), which could indicate B-field diffusion to the surface (see Ho 2011).

4. CONCLUSIONS

We present an X-ray study of all isolated radio pulsars within 100 pc of the Galactic plane, which has spin-down-inferred B-fields weaker than $10^{11}\,\mathrm{G}$, with the aim of searching for CCO-like thermal X-ray emission. None of our 12 candidates were detected in the *Chandra* and *XMM-Newton* observations and we obtained bolometric luminosity limits of 10^{32}–$10^{34}\,\mathrm{erg\,s^{-1}}$. The limits were compared with a standard neutron star cooling model to constrain the source ages. Together with the lack of known associated SNRs, we conclude that all candidates are unlikely to be young CCOs. This result supports the idea that young CCOs and currently known weak-field radio pulsars are not connected through evolution. This could be a consequence of field burial by supernova materials. We model the pulsar spin evolution in this scenario and show that the surface B-field could reemerge rapidly with a timescale shorter than 100 kyr. It could therefore be fruitful to include radio pulsars with slightly stronger fields ($B \sim 10^{11}\,\mathrm{G}$) in future searches for CCO descendants.

REFERENCES

Akmal, A., Pandharipande, V. R., & Ravenhall, D. G. 1998, PhRvC, 58, 1804
Allen, G. E., Chow, K., DeLaney, T., et al. 2015, ApJ, 798, 82
Archibald, A. M., Bogdanov, S., Patruno, A., et al. 2015, ApJ, 807, 62

Becker, W., Prinz, T., Winkler, P. F., & Petre, R. 2012, ApJ, 755, 141
Bhattacharya, D., Wijers, R. A. M. J., Hartman, J. W., & Verbunt, F. 1992, A&A, 254, 198
Bogdanov, S. 2014, ApJ, 790, 94
Bogdanov, S., Ng, C.-Y., & Kaspi, V. M. 2014, ApJL, 792, L36

Bonanno, A., Urpin, V., & Belvedere, G. 2006, A&A, 451, 1049
Cassam-Chenaï, G., Decourchelle, A., Ballet, J., et al. 2004, A&A, 427, 199
Chevalier, R. A. 1989, ApJ, 346, 847
de Luca, A. 2008, in AIP Conf. Proc., 983, 40 Years of Pulsars: Millisecond Pulsars, Magnetars and More, ed. C. Bassa, Z. Wang, A. Cumming, & V. M. Kaspi (Melville, NY: AIP), 311
Espinoza, C. M., Lyne, A. G., Kramer, M., Manchester, R. N., & Kaspi, V. M. 2011, ApJL, 741, L13
Faucher-Giguère, C.-A., & Kaspi, V. M. 2006, ApJ, 643, 332
Fesen, R. A., Kremer, R., Patnaude, D., & Milisavljevic, D. 2012, AJ, 143, 27
Fesen, R. A., Hammell, M. C., Morse, J., et al. 2006, ApJ, 645, 283
Freeman, P., Doe, S., & Siemiginowska, A. 2001, Proc. SPIE, 4477, Astronomical Data Analysis, ed. J.-L. Starck & F. D. Murtagh, 76
Gaensler, B. M., Tanna, A., Slane, P. O., et al. 2008, ApJL, 680, L37
Geppert, U., Page, D., & Zannias, T. 1999, A&A, 345, 847
Gnedin, O. Y., Yakovlev, D. G., & Potekhin, A. Y. 2001, MNRAS, 324, 725
Gotthelf, E. V., & Halpern, J. P. 2008, in AIP Conf. Proc., Vol. 983, 40 Years of Pulsars: Millisecond Pulsars, Magnetars and More, ed. C. Bassa, Z. Wang, A. Cumming, & V. M. Kaspi (Melville, NY: AIP), 320
Gotthelf, E. V., Halpern, J. P., & Alford, J. 2013a, ApJ, 765, 58
Gotthelf, E. V., Halpern, J. P., Allen, B., & Knispel, B. 2013b, ApJ, 773, 141
Gotthelf, E. V., Perna, R., & Halpern, J. P. 2010, ApJ, 724, 1316
Gudmundsson, E. H., Pethick, C. J., & Epstein, R. I. 1982, ApJL, 259, L19
Halpern, J. P., Bogdanov, S., & Gotthelf, E. V. 2013, ApJ, 778, 120
Halpern, J. P., & Gotthelf, E. V. 2010, ApJ, 709, 436
Harding, A. K. 2013, Frontiers of Physics, 8, 679
He, C., Ng, C.-Y., & Kaspi, V. M. 2013, ApJ, 768, 64
Heinke, C. O., & Ho, W. C. G. 2010, ApJL, 719, L167
Ho, W. C. G. 2011, MNRAS, 414, 2567
Ho, W. C. G. 2013a, in IAU Symp. 291, Neutron Stars and Pulsars: Challenges and Opportunities after 80 years, ed. J. van Leeuwen, 101
—. 2013b, MNRAS, 429, 113

Ho, W. C. G., Elshamouty, K. G., Heinke, C. O., & Potekhin, A. Y. 2015, PhRvC, 91, 015806
Kargaltsev, O., Pavlov, G. G., Sanwal, D., & Garmire, G. P. 2002, ApJ, 580, 1060
Kaspi, V. M. 2010, PNAS, 107, 7147
Keane, E. F., & Kramer, M. 2008, MNRAS, 391, 2009
Klochkov, D., Suleimanov, V., Pühlhofer, G., et al. 2015, A&A, 573, A53
Kramer, M., Bell, J. F., Manchester, R. N., et al. 2003, MNRAS, 342, 1299
Lazendic, J. S., Slane, P. O., Gaensler, B. M., et al. 2003, ApJL, 593, L27
Lovchinsky, I., Slane, P., Gaensler, B. M., et al. 2011, ApJ, 731, 70
Manchester, R. N., Hobbs, G. B., Teoh, A., & Hobbs, M. 2005, AJ, 129, 1993
McClure-Griffiths, N. M., Green, A. J., Dickey, J. M., et al. 2001, ApJ, 551, 394
Merloni, A., Predehl, P., Becker, W., et al. 2012, arXiv:1209.3114
Muslimov, A., & Page, D. 1996, ApJ, 458, 347
Ng, C.-Y., Romani, R. W., Brisken, W. F., Chatterjee, S., & Kramer, M. 2007, ApJ, 654, 487
Page, D., Geppert, U., & Weber, F. 2006, NuPhA, 777, 497
Park, S., Kargaltsev, O., Pavlov, G. G., et al. 2009, ApJ, 695, 431
Pavlov, G. G., Sanwal, D., & Teter, M. A. 2004, IAU Symp. 218, Young Neutron Stars and Their Environments, ed. F. Camilo & B. M. Gaensler (San Francisco: ASP), 239
Potekhin, A. Y., Yakovlev, D. G., Chabrier, G., & Gnedin, O. Y. 2003, ApJ, 594, 404
Roger, R. S., Milne, D. K., Kesteven, M. J., Wellington, K. J., & Haynes, R. F. 1988, ApJ, 332, 940
Shabaltas, N., & Lai, D. 2012, ApJ, 748, 148
Spruit, H. C. 2008, in AIP Conf. Proc. 983, 40 Years of Pulsars: Millisecond Pulsars, Magnetars and More, ed. C. Bassa, Z. Wang, A. Cumming, & V. M. Kaspi (Melville, NY: AIP), 391
Stappers, B. W., Archibald, A. M., Hessels, J. W. T., et al. 2014, ApJ, 790, 39
Sun, M., Seward, F. D., Smith, R. K., & Slane, P. O. 2004, ApJ, 605, 742
Viganò, D., & Pons, J. A. 2012, MNRAS, 425, 2487
Viganò, D., Rea, N., Pons, J. A., et al. 2013, MNRAS, 434, 123
Yakovlev, D. G., & Pethick, C. J. 2004, ARA&A, 42, 169